Effect of Creep Strain on the Optomechanical Properties and Some Structural Properties of Terylene Fibers

E. A. Seisa

Physics Department, Faculty of Science, Mansoura University, Mansoura, Egypt

Received 5 April 2008; accepted 21 January 2009
DOI 10.1002/app.30101
Published online 19 March 2009 in Wiley InterScience (www.interscience.wiley.com).

ABSTRACT: This article sheds light on the effect of creep strain [$\varepsilon(t)$; %] on the optomechanical properties and some structure properties of terylene fibers at several constant applied loads. Automated multiple-beam Fizeau fringes in transmission were used with a mechanical creep device attached to a wedge interferometer where the fiber was subjected to a constant load. This technique was used to determine the mean refractive indices and the mean birefringence values of terylene fibers under different conditions of $\varepsilon(t)$. The obtained optical results were used to evaluate the optical orientation function, optical stress coefficient, density, crystallinity, and mean-square density fluctuation with $\varepsilon(t)$. The obtained results show that, under a constant load, the terylene fibers extended with time, the rate of which decreased with time. An empirical formula is suggested to represent the variation of $\varepsilon(t)$ of terylene fibers with time, and the constants of this formula were determined. A mechanical model is proposed to represent $\varepsilon(t)$ of terylene fibers, which consists of two Kelvin elements combined in series, which were used to provide an accurate fit to the experimental creep curve. The stress–strain curve via creep was studied to determine some mechanical parameters of the investigated fibers: Young's modulus, yield stress, and yield strain. Illustrations with microinterferograms, graphs, and tables are given. © 2009 Wiley Periodicals, Inc. J Appl Polym Sci 113: 516–525, 2009

Key words: creep; fibers; polyesters

INTRODUCTION

One of the methods of studying relaxation phenomena is to rapidly load a specimen and watch the course of its tensile strain (ε) under the action of the applied load, which is referred to as *creep*. One complication is that the cross section of a specimen diminishes with time, and thus, the same load produces a constantly growing stress (σ) because of the decreasing cross-sectional area.[1]

In creep experiments, σ is suddenly applied and maintained at a constant value, whereas ε is measured as a function of time. Creep involves changes in shape and dimension at a constant volume. It is one of the most important and widely used engineering tests of viscoelastic behavior. So most useful polymeric objects must be designed to withstand modest loads for long periods of time without changing shape or dimension. For example, fibers must not deform under prolonged σ, or our clothing would become undesirably misshapen.[2]

The usual explanation of creep is as follows: in the unstretched fiber, each segment of the chain molecules will be constrained by forces because of neighboring chain segments and will tend to take up a position in which its free energy is at a minimum. We may suppose that the free energy has other minima separated from the first by energy barriers and that the displacement of the chain segment due to the deformation of the fiber involves the crossing of such a barrier to one of the other minima.[3]

When the fibers are stressed, the free energy contour is deformed by a decrease in the level of the second minimum, and the position of the chain segment corresponding to this is accordingly favored. To pass over the energy barrier, however, the segment requires time, in accordance with the ordinary laws of chemical kinetics and the rate of approach to the new equilibrium depending on the heights of the free energy barriers of all of the chain segments. As more and more segments pass over their barriers, the fiber extends, and we, thus, observe the creep effect.[3]

Important information on the deformation of viscoelastic materials is obtained by creep. In the creep process, the changes in the optical properties can be determined by interferometric methods.[4,5] Interferometrics studies the optical anisotropy in some synthetic fibers as a function of the draw ratio.[6–10] The study of optical anisotropy in polymer fibers material plays an important role in the knowledge of the molecular arrangement within the fibers. Synthetic fibers in the drawn or extended state show considerable optical and mechanical anisotropy. The

Correspondence to: E. A. Seisa (seisa@mans.edu.eg).

degree of anisotropy in the drawn state is related to the amount of extension imposed.[11]

In this study, I examined the effect of creep strain [$\varepsilon(t)$; %] on the optomechanical properties and some structure properties of terylene polyester fibers at constant applied loads of 9, 12, and 15 g at room temperature. A mechanical creep device[12] attached to automated multiple-beam Fizeau fringes was used to study the variations in the optical parameters as a function of $\varepsilon(t)$ at different constant loads. Also, the orientation function, optical stress coefficient (C_s), density (ρ), degree of crystallinity (χ), and the mean-square density fluctuation ($\langle\eta^2\rangle$) at different $\varepsilon(t)$ values were determined.

THEORETICAL

Refractive indices and birefringence (Δn) values of the terylene fibers

The refractive indices in the parallel and perpendicular directions ($n^{\parallel}$ and $n^{\perp}$, respectively) and Δn values of the terylene fibers were calculated with the following equation:[11]

$$n^j = n_L + \frac{F^j\lambda}{bA} \tag{1}$$

where n^j is the refractive index in parallel or perpendicular direction ($n^{\parallel}$, $n^{\perp}$), j is the state of polarization of monochromatic light used (parallel or perpendicular) to the fiber axis, n_L is the refractive index of the immersion liquid, F^j is the area enclosed under the fringe shift, A is the mean cross-sectional area of the fiber, and b is the interfering spacing. Δn of the fiber is given by

$$\Delta n = \left(\frac{\Delta F}{b}\right)\frac{\lambda}{A} \tag{2}$$

where $\Delta F = F^{\parallel} - F^{\perp}$. Where ΔF is the value of the difference between the area enclosed by the fringe shift for light vibrating paralle. $F^{\parallel}$ and perpendicular $F^{\perp}$ to the fiber axis, respectively, and λ is the wavelength of monochromatic light used.

Determination of the optical orientation function

The optical orientation function was calculated with the following relation:[13]

$$\langle p_2(\theta)\rangle = \frac{\Delta n}{\Delta n_{\max}} = f_\Delta \tag{3}$$

which is the same function named by Hermans.[14] $p_2(\theta)$ and f_Δ are the optical orientation function. $\Delta n \supset \max$ is the maximum birefringence. The $\Delta n_{\max}$ values of terylene fibers was determined to be 0.24 by De Vries[15] for a perfectly (or fully) oriented fiber. Hermans's optical orientation function (f_θ) was corrected by De Vries to be $0 < \Delta n < 0.8$ by

$$f_\theta = (1 + a)f_\Delta - af_\Delta^2 \tag{4}$$

where the constant a is given by the equation

$$a = \frac{2n_{\parallel}^2 n_{\perp}^2}{n_v^3(n_{\parallel} + n_{\perp})} - 1 \tag{5}$$

where n_v is the virtual refractive index, which is nearly equal to the isotropic refractive index.

C_s

The value of C_s is dependent on the chemical structure of the polymer. This coefficient also depends solely on the mean refractive index ($\overline{n}$) and the optical anisotropy of the random link as seen from the following equation:[16]

$$C_S = \frac{2\pi}{45KT}\left[\frac{\left(\overline{n^2} + 2\right)^2}{\overline{n}}\right]\left[\alpha^{\parallel} - \alpha^{\perp}\right] \tag{6}$$

where K is Boltzmann's constant, T is the absolute temperature, and $\alpha^{\parallel}$ and $\alpha^{\perp}$ are the polarizabilities along and across the axis of such units, respectively. This leads to the Lorentz–Lorenz equation by the following equation:[15]

$$\frac{n_{\parallel}^2 - 1}{n_{\parallel}^2 + 2} = \frac{v\alpha^{\parallel}}{3\psi} \tag{7}$$

with analogous formula used for $n^{\perp}$ and ψ is the permittivity of free space (8.85×10^{-12} Fm^{-1}). For a bulk polymer of density ρ and monomer unit molecular weight M, the number of monomer units per unit volume is $v = N_A\rho/M$, where N_A is Avogadro's number and M (192.17) is the molecular weight of the terylene fibers.[15]

Equation of $\langle\eta^2\rangle$

For a two-phase structure consisting of amorphous and crystalline regions with densities ρ_a and ρ_c, respectively, $\langle\eta^2\rangle$ can be calculated from the following equation:[17]

$$\langle\eta^2\rangle = [\rho_c - \rho_a]^2\chi[1 - \chi] \tag{8}$$

EXPERIMENTAL

The monomer of poly(ethylene terephthalate) (PET) is related to ethylene glycol and terephthalic acid:

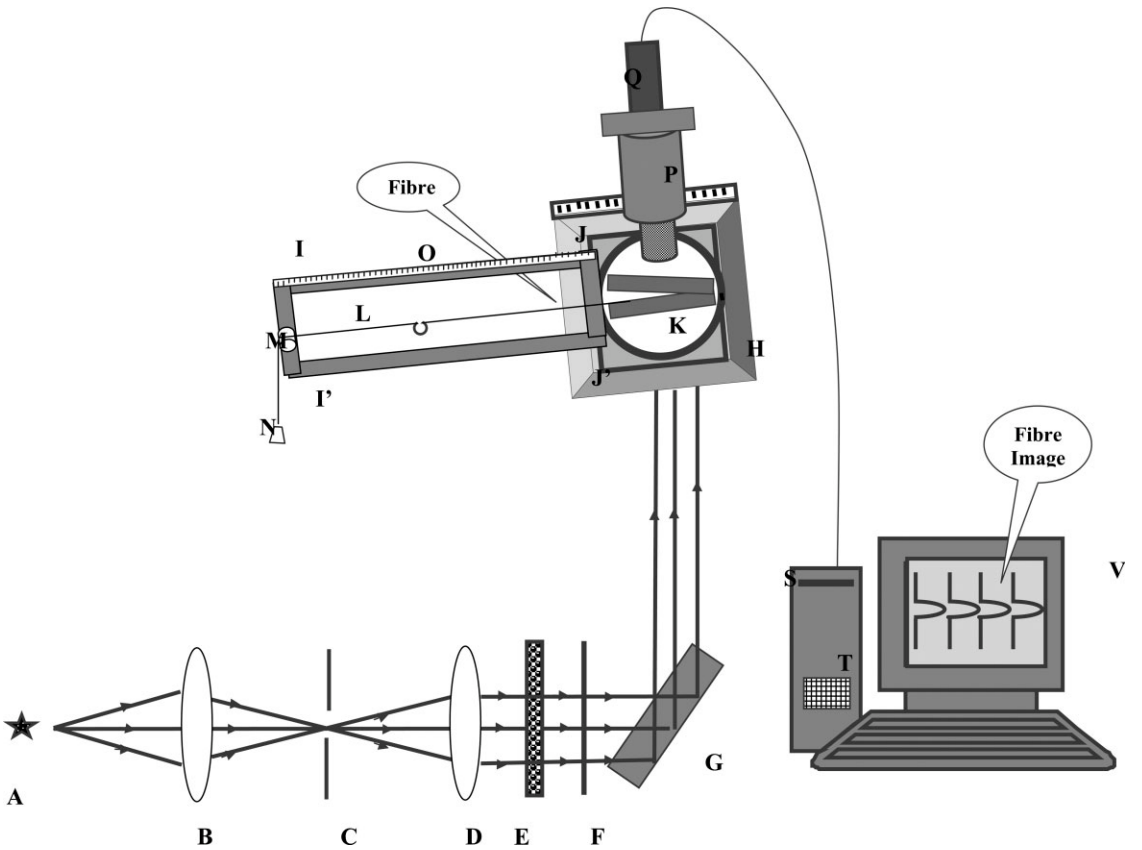

Figure 1 Schematic diagram of the mechanical creep device attached to the automated optical system for the production of multiple-beam Fizeau fringes in transmission: (A) mercury lamp, (B) condenser lens, (C) iris diaphragm, (D) collimating lens, (E) polarizer, (F) monochromatic filter, (G) reflector, (H) wedge interferometer, and (I) stretched string.

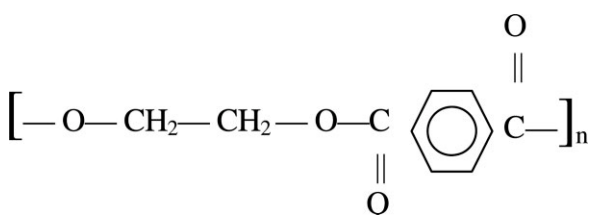

At room temperature, the undrawn material of PET is transformed to a drawn material with a constant reduction in cross section as it passes through the neck. If the drawing is a uniaxial fiber, as in the case of a fiber, the extension ratio is exactly similar to that defined for stretching a rubber.[18]

RESULTS

Figure 1 shows the optical system that was used to produce multiple-beam Fizeau fringes in transmission and a computer with a charged coupling device (CCD) camera attached.

The tested fiber was fixed on the lower silvered circular optical flat, and the other end was linked to a stretched string. The string was run freely on the surface of the smooth wheel under several constant loads. A few drops of an immersion liquid were put on the fixed fiber, and another silvered circular optical flat placed on it to form a wedge interferometer was fixed on the movable microscope stage. A mechanical creep device[5] was connected to a wedge interferometer to produce fiber interference patterns. A parallel beam of monochromatic light of wavelength 546.1 nm was incident normal to the wedge interferometer. The interference fringe shift due to the difference in the fiber and liquid refractive indices was obtained. The fiber images (microinterferogram) captured with the CCD camera were used to determine the $\overline{n}$ values and mean Δn of terylene fibers at each value of $\varepsilon(t)$ under several constant applied loads.

Three samples of undrawn terylene fibers (draw ratio = 1) with circular cross-sectional areas of mean value 1352.78 μm^2 were investigated. The initial fiber length was 13 cm, and each sample was elongated for a duration of 150 min under several constant applied loads of 9, 12, and 15 g at room temperature.

Figure 2(a–d) shows the microinterferograms of multiple-beam Fizeau fringes in transmission for light vibrating parallel and perpendicular to fiber axis of the terylene fibers at a constant applied load

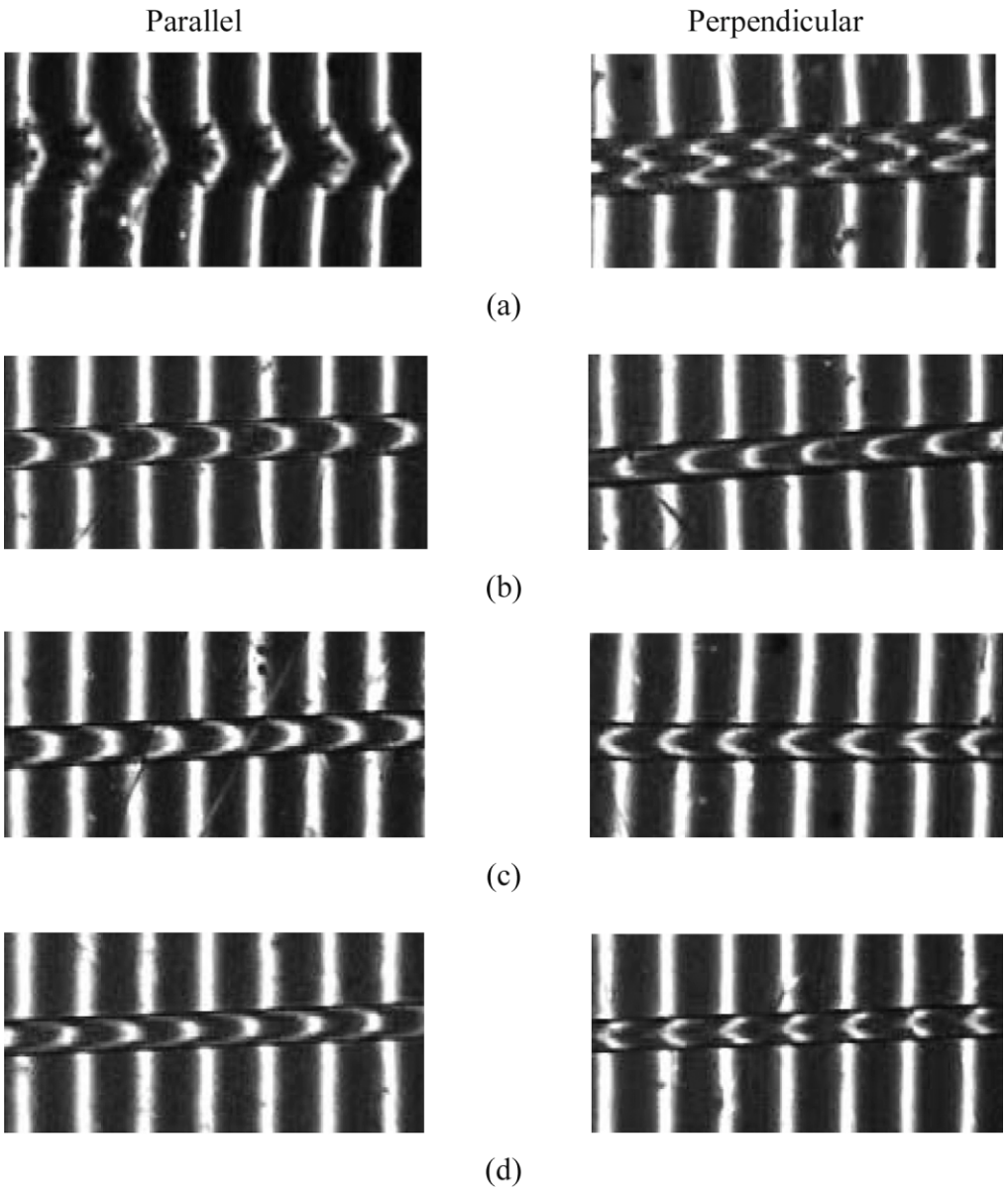

Figure 2 Microinterferograms of multiple-beam Fizeau fringes in transmission for light vibrating parallel and perpendicularly to the fiber axis of the terylene fibers at a constant applied load of 12 g. The $\varepsilon(t)$ values were (a) 0, (b) 51.85, (c) 96.30, and (d) 185.19%.

of 12 g. The $\varepsilon(t)$ values for the interferograms [Fig. 2(a–d)] were 0, 51.85, 96.30, and 185.19%, respectively. Monochromatic light of wavelength 546.1 nm was used, and the refractive index of the immersion liquid was 1.546 ± 0.0004 at 22°C. The fringe shifts in the microinterferograms identified the differences in optical path variations due to increasing $\varepsilon(t)$. They also showed the appearance of different shifts at different states of stretching (creep).

Figure 3 shows the schematic representation of different states of creep deformation of the tested fiber in the long run. Figure 3(a) represents the unstressed specimen of the terylene fibers and corresponds to the microinterferogram in Figure 2(a). Figure 3(b) shows the first slight reduction in the diameter and corresponds to the microinterferogram in Figure 2(b). Figure 3(c) shows the starting formation of the neck, as in Figure 2(c). Figure 3(d) shows more stretching for the fiber and corresponds to the microinterferogram in Figure 2(d).

Also, a gradual decrease in fiber diameter and changes in the fringe shifts were observed. The variation of A of the fibers with $\varepsilon(t)$ is shown in Figure 4. There was an initially rapid decrease of A with $\varepsilon(t)$, and a decrease occurred more slowly with increasing ε. The creep study was conducted under conditions of constant σ and ε measured as a function of time t.

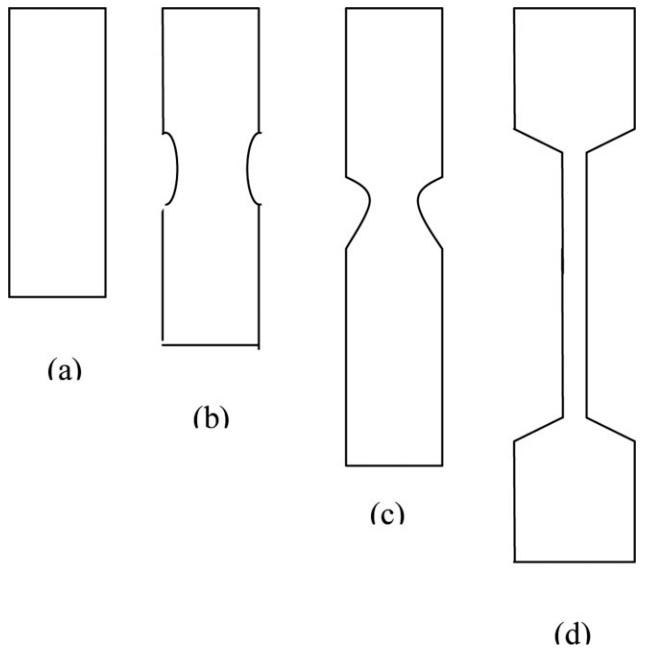

Figure 3 Schematic representations of the different states of creep deformation of the fiber: (a) initial specimen, (b) insignificant reduction in A due to the increase in overall length, (c) beginning of the formation of a neck, and (d) the entire specimen passing into the neck except for the part at the fixed end.

Experimental description of the creep behavior of the terylene fibers

Figure 5(a) shows the variation of $\varepsilon(t)$ with time under various mechanical loads of terylene fibers. It was clear that, when the fiber subjected to a constant load, its ε was a function of the time. $\varepsilon(t)$ initially decreased with ε (primary creep); then, it remained constant with further increases in ε (secondary creep), as shown in Figure 5(b). It was obvious that the rate of ε decreased as time increased but may never have actually decreased to zero.[3]

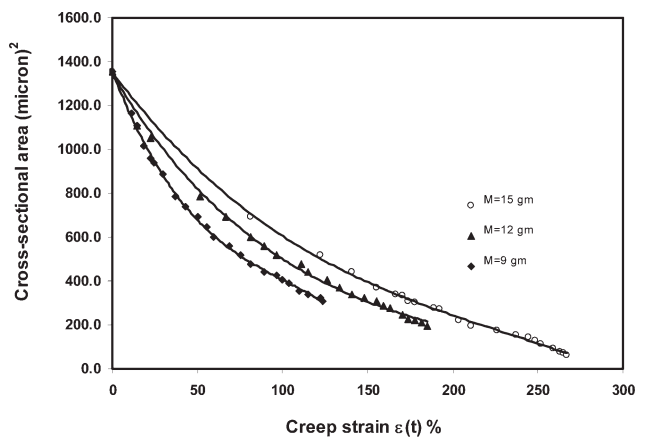

Figure 4 Variation of A of the terylene fibers as function of $\varepsilon(t)$ at various constant loads of 9, 12, and 15 g.

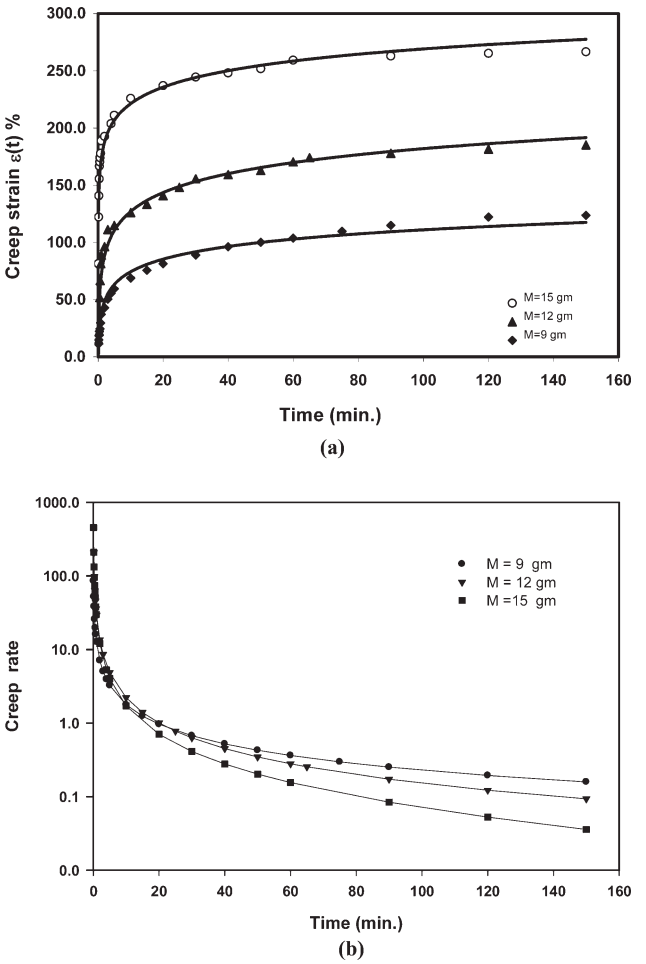

Figure 5 (a) $\varepsilon(t)$ as a function of time of the terylene fibers at various constant loads of 9, 12, and 15 g and (b) creep rate as a function of time.

A good description of the experimental values of $\varepsilon(t)$ for the terylene fibers was obtained from our suggested empirical relation

$$\varepsilon(t) = a(1 - e^{-bt}) + c(1 - e^{-dt}) \tag{9}$$

where a, b, c, and d are empirical constants, which were determined and are listed in Table I.

The experimentally determined $\varepsilon(t)$ for terylene fiber was fitted by means of a proposed mechanical model, which consists of a combination of the two Kelvin elements in series (the elastic element represented by a spring and the viscous element represented by a dashpot), as shown on Figure 6. This

TABLE I
Values of the Constants in eq. (9) for the Terylene Fibers

	Constant			
M (g)	a (GPa^{-1})	b (S^{-1})	c (GPa^{-1})	d (S^{-1})
9	48.7651	1.2847	74.6306	0.0253
12	105.9753	1.3276	78.444	0.0293
15	179.6009	6.3412	80.5426	0.0709

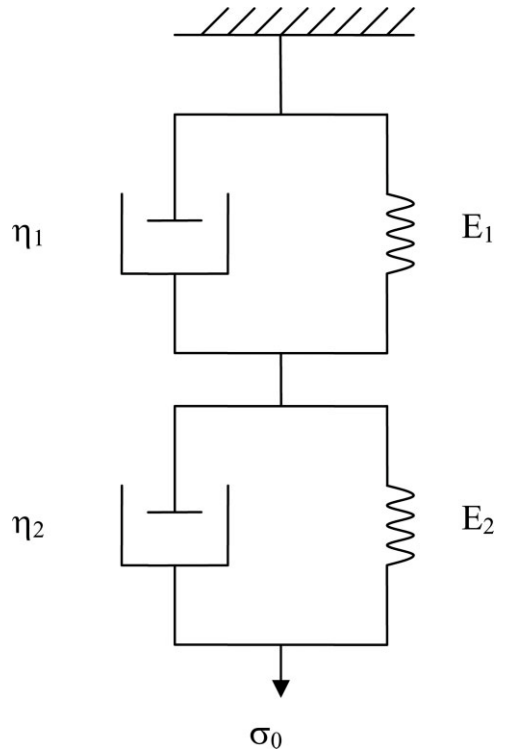

Figure 6 Two-Kelvin model in series.

model shows a creep curve similar to those represented in Figure 5(a) for terylene fiber. $\varepsilon(t)$ changes with time under a constant load according to the following equation, which was given by Ward and Hadley:[18]

$$\varepsilon(t) = \frac{\sigma_0}{E_1}(1 - e^{-t/\tau_1}) + \frac{\sigma_0}{E_2}(1 - e^{-t/\tau_2}) \qquad (10)$$

where σ_o is the constant static engineering stress applied to the specimen during creep, E_1 and E_2 are the spring moduli, $\tau_1 = \eta_1/E_1$, and $\tau_2 = \eta_2/E_2$ are the retardation times, and η_1 and η_2 are the dashpot viscosities. The values of E_1, E_2, τ_1, τ_2, η_1, and η_2 were determined from the corresponding constants *a, b, c*, and *d* given by eq. (9). The results were tabulated in Table II.

For the two-Kelvin model in series, when a constant load is applied, the initial elongation comes from the springs with moduli E_1 and E_2. Later elongation comes from the movement of dashpots with viscosities η_1 and η_2. The total elongation of the model is the sum of the individual elongation of the two parts. The change of the elongation with time is given by eq. (10). The correlation between the experimental data and model prediction was suitable.

Influence of $\varepsilon(t)$ on the optical properties of the terylene fibers

The refractive index is the major physical quantity that links the optical and structural properties of any fiber. So the experimental values of the mean $n^{\parallel}$ and $n^{\perp}$ and mean Δn of the terylene fibers at each value of $\varepsilon(t)$ under different constant loads of 9, 12, and 15 g at room temperature were determined with eq. (1).

Figure 7 shows the variation of the mean $n^{\parallel}$ and $n^{\perp}$ with $\varepsilon(t)$ at different constant loads. As $\varepsilon(t)$ increased, $n^{\parallel}$ increased, but $n^{\perp}$ decreased. This behavior means that, during $\varepsilon(t)$, the fiber chains became oriented in the direction of extension (parallel to the fiber axis). Δn is an important physical parameter that links the optical and mechanical properties of fiber. The variation of the mean Δn with $\varepsilon(t)$ is shown in Figure 8. It is clear that the mean Δn increased with increasing $\varepsilon(t)$. This means that more orientation occurred involving molecular arrangements in both the crystalline and in amorphous regions.

The optical results of $n^{\parallel}$, $n^{\perp}$, and Δn of the terylene fibers were used to calculate the optical orientation function, C_s, ρ, χ, and $\langle\eta^2\rangle$ at different values of $\varepsilon(t)$.

Figure 9 shows the relationship between the optical orientation [$f(\theta)$] and $\varepsilon(t)$ of terylene fibers at different mechanical loads. As $\varepsilon(t)$ increased, $f(\theta)$ increased. The higher the orientation factor was, the more mutually parallel the molecules were and the smaller the average angle formed by them was within the fiber axis. Also, the optical orientation function decreased as the mechanical load increased; this means that the fiber material became less oriented.

Figure 10 shows the relation between C_s with $\varepsilon(t)$ of the terylene fibers at different constant loads. An increase in the C_s values resulted from increasing $\varepsilon(t)$.

TABLE II
Values of σ_o, E_1 and E_2, τ_1 and τ_2, and η_1 and η_2 Given in the Proposed Kelvin Chain for the Terylene Fibers Under Constant Loads of 9, 12, and 15 g

	Constant						
M (g)	σ_o (GPa)	E_1 (GPa)	E_2 (GPa)	τ_1 (s)	τ_2 (s)	η_1 (GPa s)	η_2 (GPa s)
9	0.0652	0.0013	0.0009	0.7784	39.5257	0.0010	0.0346
12	0.0870	0.0008	0.0011	0.7532	34.1297	0.0006	0.0378
15	0.1087	0.0006	0.0013	0.1577	14.104	0.0001	0.0190

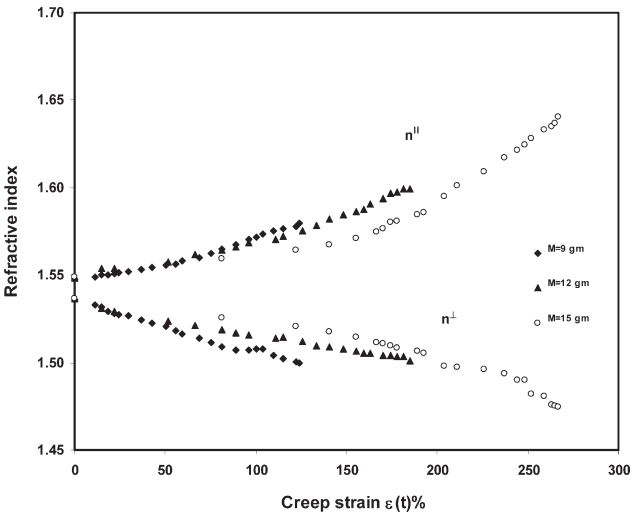

Figure 7 Variation of the mean $n^{\parallel}$ and $n^{\perp}$ of the terylene fibers as a function of $\varepsilon(t)$ at various constant loads of 9, 12, and 15 g.

Evaluation of ρ and χ

ρ is the most basic macroscopic quantity of a crystal. It is linked directly to the unit cell parameters. ρ can be measured by a different number of methods, which have different techniques, that is, the ρ gradient, dilatometer, and vibrating string for fibers.[19,20]

So to explain this study and evaluate χ, I found that this described calculations for the ρ and χ and was an available technique in our laboratory.

ρ was calculated from the mean isotropic refractive index (n_{iso}) with the Lorentz–Lorenz equation:[21]

$$\rho = \rho_i \left(\frac{\overline{n^2} - 1}{\overline{n^2} + 2}\right)\left(\frac{n_{iso}^2 + 2}{n_{iso}^2 - 1}\right) \tag{11}$$

where $\rho_i = \rho_a = 1.336 \times 10^3$ kg/m^3 is the density of the amorphous phase for the terylene fibers.

n_{iso} was deduced from the measured values of $n^{\parallel}$ and $n^{\perp}$ with the following well-known equation:[19]

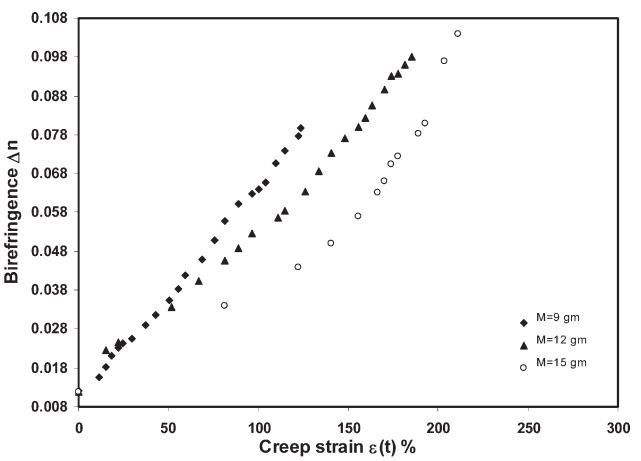

Figure 8 Variation of the mean Δn with $\varepsilon(t)$.

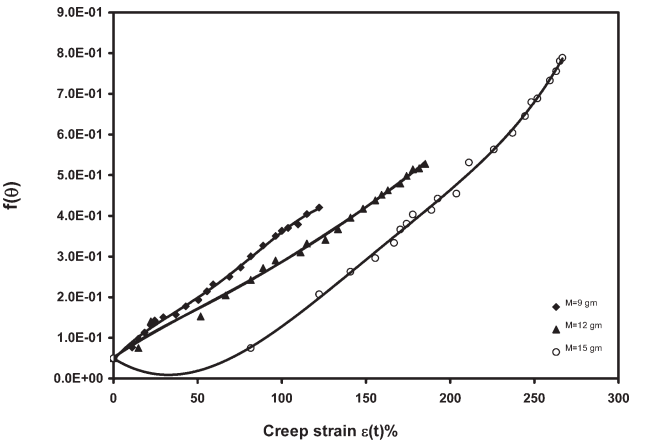

Figure 9 Relationship between $f(\theta)$ of the terylene fibers and $\varepsilon(t)$.

$$n_{iso} = (n^{\perp 2} n^{\parallel})^{1/3} \tag{12}$$

χ was determined from the following equation by the well-known relation of ρ:[22]

$$\chi = \frac{\rho_c(\rho - \rho_a)}{\rho(\rho_c - \rho_a)} \times 100 \tag{13}$$

where $\rho_c = 1.457 \times 10^3$ kg/m^3 is the density of the crystalline phase of the terylene fibers. The slight change in n_{iso} (Table III) denoted a change in volume resulting from mass redistribution associated with the creep process. This change in volume affected other parameters, such as ρ and χ. Figure 11(a,b) shows the relationships between $\varepsilon(t)$ for the terylene fibers and ρ and χ, respectively, at different mechanical loads. Both ρ and χ increased with increasing $\varepsilon(t)$ but decreased with increasing mechanical loads.

The relation between $\langle \eta^2 \rangle$ of the terylene fibers and $\varepsilon(t)$ is shown in Figure 12.

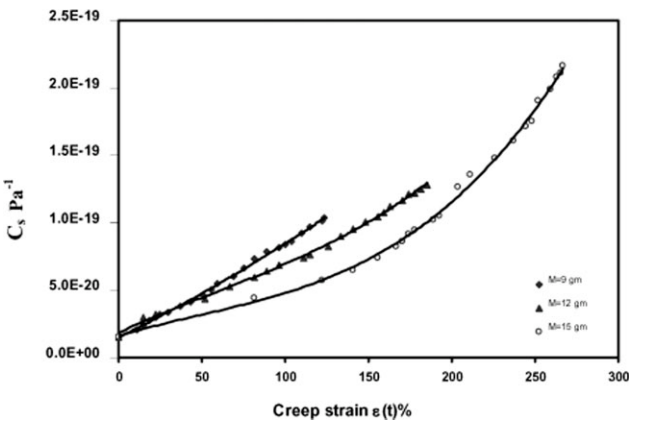

Figure 10 Relationship between the C_s values of the terylene fibers with $\varepsilon(t)$.

TABLE III
Values of n_{iso} at Different Values of $\varepsilon(t)$ for the Terylene Fibers Under Constant Loads of 9, 12, and 15 g

$M = 9$ g		$M = 12$ g		$M = 15$ g	
$\varepsilon(t)$ (%)	n_{iso}	$\varepsilon(t)$ (%)	n_{iso}	$\varepsilon(t)$ (%)	n_{iso}
0.00	1.5399	0.00	1.5406	0.00	1.5408
24.44	1.5352	81.48	1.5338	166.7	1.5322
50.37	1.5321	114.81	1.5334	188.9	1.5321
75.56	1.5282	148.15	1.5329	225.9	1.5330
100.00	1.5285	170.37	1.5335	251.9	1.5293
122.22	1.5259	185.19	1.5329	266.7	1.5279

Influence of $\varepsilon(t)$ on some mechanical parameters

The σ–ε curve due to creep is one useful relationship that provides the stability of deformation and some mechanical properties for terylene fibers. The variation of the interferometry pattern on the CCD was captured during the creep process. The obtained microinterferograms were used to determine the diameter and, hence, the A values of the fibers. The way the resulting changes in the A values of the fibers affected the actual σ is

$$\sigma = F/A \tag{14}$$

where $F = Mg$ is the applied tensile force, M is the mass (load), and g is the acceleration due to gravity. The elongation (ε) of fibers can be calculated by

$$\varepsilon = \frac{L - L_0}{L_0} \tag{15}$$

where L and L_0 are the lengths of the sample after and before deformation, respectively. The σ and ε curve of the terylene fibers is shown in Figure 13.

From this curve, Young's modulus (E) is equal to the slope of the σ–ε curve at the origin and is a measure of the resistance of elongation before the yield point.[23] The yield point determines the intersection of the tangent at the origin with the tangent having the least slope; the results are listed in Table IV. It is clear that E decreased, whereas yield stress (σ_y) and yield strain (ε_y) increased for the terylene fibers with increased loads.

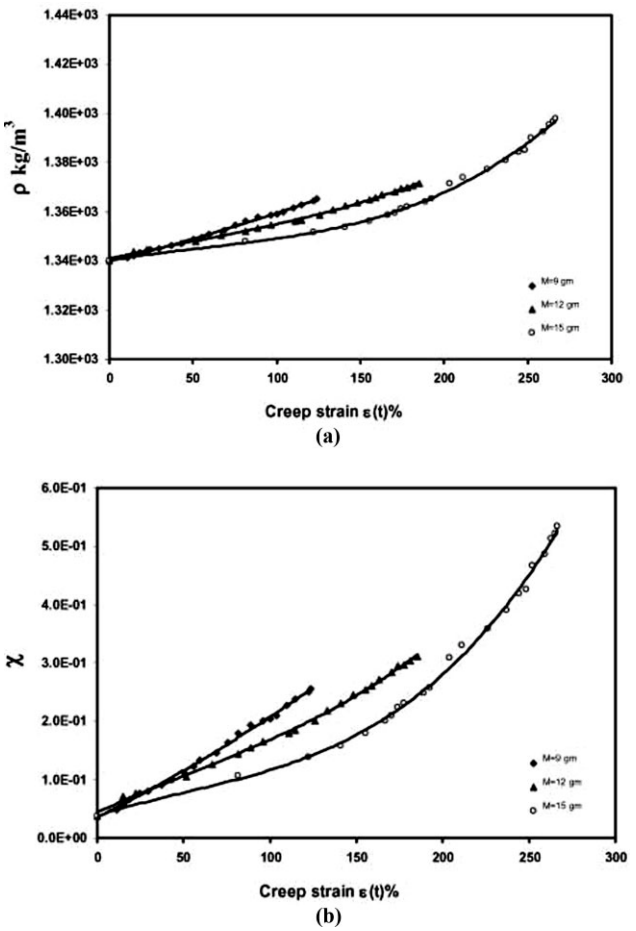

Figure 11 Relationship between (a) ρ and (b) χ of the terylene fibers as a function of $\varepsilon(t)$ at various constant loads of 9, 12, and 15 g.

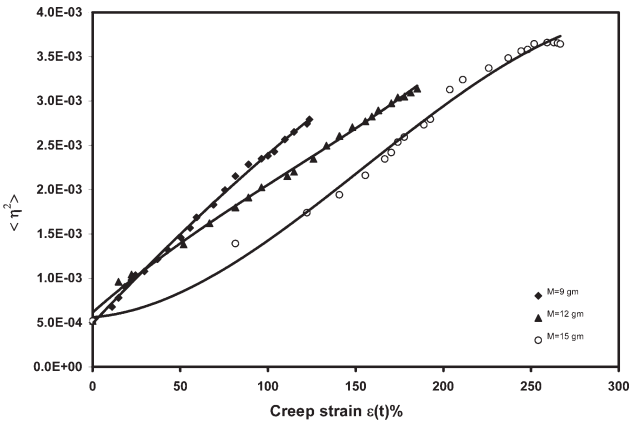

Figure 12 Relationship between $\langle\eta^2\rangle$ of the terylene fibers and $\varepsilon(t)$.

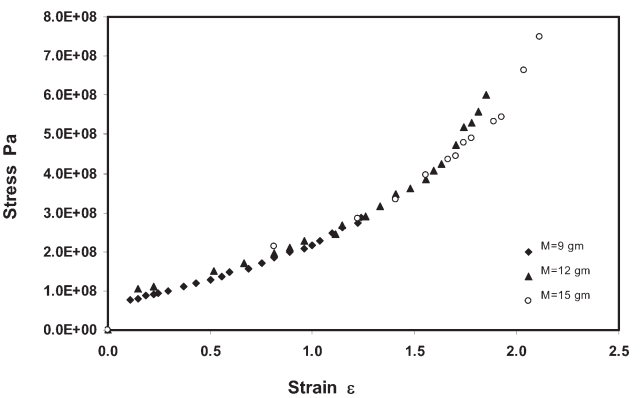

Figure 13 σ–ε curve via creep for the terylene fibers under constant loads of 9, 12, and 15 g.

TABLE IV
***E*, σ_y, and ε_y for the Terylene Fibers at Various Loads**

M (g)	*E* (GPa)	σ_y (GPa)	ε_y
9	0.608	0.090	0.148
12	0.596	0.115	0.193
15	0.453	0.145	0.320

DISCUSSION

Deformation due to creep processes is the predominant means of producing new physical structures of polymeric fibers, which are so important commercially and are of much industrial interest. The determination of the properties of the polymers and fibers was done by various treatments: mechanical, thermal, chemical, and others. By means of the creep process, the development of the properties was due to changes in the molecular arrangement, and hence, the creation of a new structure that tended to change the polymeric properties was expected. The creep process produces an orientation that helps one gain greater insight at the microstructure level when investigating mechanical properties. The orientation has a pronounced effect on the physical properties of polymers. Δn, or changes in the index or refraction with direction of a crystalline polymer made up of contributions from crystalline and amorphous regions plus a contribution from Δn, results from the shape of the crystals or the presence of voids, as shown in Figures 7–9. For a completely unoriented material, the contributions of both the crystalline and amorphous regions are zero. The increase in Δn on orientation was due to the crystalline regions and was proportional to χ and an orientation factor, as shown in Figures 8 and 9.

Generally, the evaluation of χ from ρ data according to eq. (13) and the interpretation of physical properties of semicrystalline polymers are based on a two-phase model, which agrees with the proposed mechanical model consisting of two Kelvin elements combined in series (Fig. 6). It is the simplest model that exhibits all the essential features of viscoelasticity; on the application of σ_o, the model suggests an elastic deformation, followed by creep, as shown in Figure 5(a). In this, it is assumed that the polymer consists of an amorphous and a crystalline phase and that the properties of each phase are independent of the presence and amount of the other phase. This assumption also involves a certain conception of the development of the morphological structure. Because of the importance of the idea of a two-phase structure, it is worth checking its validity. A suitable method for this purpose is to calculate the mean ρ fluctuation for a two-phase structure consisting of amorphous and crystalline regions with densities ρ_a and ρ_c, respectively.

The value of C_s depends on the chemical structure of the polymer and is somehow temperature dependent. The theory of rubber elasticity leads to eq. (6). According to theory, C_s is independent of the degree of crosslinking. During σ, relaxation Δn decreases; the same is true during creep.[24]

CONCLUSIONS

Form the measurements carried out for terylene fibers, when this fiber was subjected to $\varepsilon(t)$ at room temperature, the following conclusions were drawn:

1. Creep rates were initially very high but decayed rapidly with time increase for all applied loads [Fig. 5(b)], but may have never actually decreased to zero.
2. The refractive index of the fiber $n^{\parallel}$ and its Δn increased with increasing $\varepsilon(t)$ (Figs. 7 and 8). This means that the polymer molecules tend to be aligned parallel to the fiber axis as the fiber is subjected to creep, and one might relate $\varepsilon(t)$ to the tensile properties of these fibers.
3. The obtained principal optical parameters and χ were suitable for evaluating the orientation function, C_s, and $\langle \eta^2 \rangle$.
4. Changes in the cross-sectional area indicated a change in the specific volume and mass redistribution of terylene fibers due to the creep process (Fig. 4), and the microinterferograms clearly identified a difference in optical path variations due to $\varepsilon(t)$ of the terylene fibers (Fig. 2).
5. The application of automatic multiple-beam Fizeau fringes in transmission was a useful tool for monitoring the changes in the structure of terylene fibers during the creep process.

We conclude from the previous results and considerations that the practical importance of these measurements is that they provide acceptable results for the optocreep parameters. Because changes in the optical parameters were a consequence of the material creep process, the reorientation of terylene fibers may occur not only during fabrication but also after the fabrication process.

Also, the multiple-beam technique is very promising for revealing changes due to any physical deformation processes for studying the optical behavior of the structure of any polymeric fiber. Also, the textile industry is interested in these optical methods as a nondestructive quality control techniques to determine the onset of creep deformation.

The author expresses her gratitude and appreciation to I. M. Fouda and K. A. El-Farahaty for useful discussion.

References

1. Kuleznev, V. N.; Shershnev, V. A. The Chemistry and Physics of Polymers; Mir: Moscow, 1990.
2. Williams, D. J. Polymer Science and Engineering; Prentice-Hall: Upper Saddle River, NJ, 1971.
3. Woods, H. J. Physics of Fibers; Institute of Physics: London, 1955.
4. El-Farahaty, K. A. J Appl Polym Sci 1998, 67, 621.
5. Fouda, I. M.; El-Farahaty, K. A.; Seisa, E. A. J Appl Polym Sci 2008, 110, 761.
6. Fouda, I. M.; Seisa, E. A. J Appl Polym Sci 2007, 106, 1768.
7. Fouda, I. M.; El-Khodary, A.; El-Sharkawy, F. M. Int J Polym Mater 2007, 56, 965.
8. Seisa, E. A. Int Polym Process 2006, 21, 183.
9. Fouda, I. M.; Seisa, E. A. J Polym Res 2008, 15, 259.
10. Ward, I. M. Structure and Properties of Orientated Polymers; Applied Science: London, 1975.
11. Barakat, N.; Hamza, A. A. Interferometry of Fibrous Materials; Hilger: Bristol, United Kingdom, 1990.
12. El-Farahaty, K. A. Polym Test 1996, 15, 163.
13. Ward, I. M. J Polym Sci Polym Symp 1977, 53, 9.
14. Hermans, P. H. Contribution to the Physics of Cellulose Fiber; North-Holland: Amsterdam, 1946.
15. De Vries, H. Z Colloid Polym Sci 1979, 257, 226.
16. Riande, E.; Guzman, J. J Polym Sci Polym Phys Ed 1984, 22, 917.
17. Fischer, E. W.; Fakirov, S. J Mater Sci 1976, 11, 1041.
18. Ward, I. M.; Hadley, D. W. An Introduction to the Mechanical Properties of Solid Polymers; Wiley: New York, 1993.
19. Bernhard, W. Macromolecular Physics, Crystal Structure, Morphology and Defects; Academic: New York, 1973.
20. Fouda, I. M. J Polym Res 2002, 9, 37.
21. De Vries, H.; Bonnebat, C.; Beautemps, J. J Polym Sci Polym Symp 1977, 58, 109.
22. Griskey, R. G. Polymer Process Engineering; Chapman & Hall: London, 1995.
23. Morton, W. E.; Hearls, J. W. S. Physical Properties of Textile Fibers; Butterworths: London, 1962.
24. Van Krevelen, D. W.; Hoftyzer, P. J. Properties of Polymer: Their Estimation and Correlation with Chemical Structure, 2nd ed.; Elsevier: Oxford, 1976.